

Bandgap bowing in BGaN thin films

A. Ougazzaden,^{1,a)} S. Gautier,² T. Moudakir,² Z. Djebbour,³ Z. Lochner,⁴ S. Choi,⁴ H. J. Kim,⁴ J.-H. Ryou,⁴ R. D. Dupuis,⁴ and A. A. Sirenko^{5,b)}

¹Georgia Institute of Technology/GTL, UMI 2958 GT-CNRS, 2-3 Rue Marconi F-57070 Metz, France

²Laboratoire Matériaux Optiques, Photonique et Système (LMOPS), UMR CNRS 7132, University of Metz and Supélec, 2 Rue E. Belin F-57070 Metz, France

³Department of Physics and Engineering Science, University of Versailles UVSQ, 45 Av. Des Etats Unis, 78035 Versailles, France and LGEP, UMR 8507 CNRS, SUPELEC, University Paris-Sud 11, University Pierre et Marie Curie, 11 Rue Joliot Curie, 91192 Gif-sur-Yvette, France

⁴Center for Compound Semiconductors and School of Electrical and Computer Engineering, Georgia Institute of Technology, Atlanta, Georgia 30332, USA

⁵Department of Physics, New Jersey Institute of Technology, Newark, New Jersey 07102, USA

(Received 16 June 2008; accepted 13 August 2008; published online 28 August 2008)

We report on the bandgap variation in thin films of $B_xGa_{1-x}N$ grown on AlN/sapphire substrates using metal-organic vapor phase epitaxy. Optical transmission, photoluminescence, and x-ray diffraction were utilized to characterize the materials' properties of the $B_xGa_{1-x}N$ films. In contrast to the common expectation for the bandgap variation, which is based on the linear interpolation between the corresponding GaN and BN values, a significant bowing ($C=9.2\pm 0.5$ eV) of the bandgap was observed. A decrease in the optical bandgap by 150 meV with respect to that of GaN was measured for the increase in the boron composition from 0% to 1.8%. © 2008 American Institute of Physics. [DOI: 10.1063/1.2977588]

Ternary and quaternary layers of nitrides are important for bandgap engineering of GaN-based optoelectronic devices. The introduction of boron, which is a “light” element, could, in principle, compensate for the strain induced by a high fraction of “heavy” indium in InGaN-based light emitters and could provide lattice matching for BGaN grown on AlN and SiC substrates. BGaN is a new material and its basic electronic and structural properties are not well known. One expects a decrease in the lattice parameters with the increasing fraction of boron and a natural increase in the bandgap E_g compared to that for GaN, as it has been predicted by Harrison.¹ In accordance with the quantum dielectric theory,² the bandgap of wurtzite (w) $B_xGa_{1-x}N$ increases with boron content x . This trend had been experimentally observed using photoluminescence (PL) and optical reflectivity for BGaN grown directly on 6H-SiC substrates by using metal-organic vapor phase epitaxy (MOVPE) for a range of $x < 1\%$.³ However, effects of a possible residual strain in the layers studied in Ref. 3, which may result in a blueshift of the PL peaks, had not been decoupled from the composition-induced variation for the bandgap of BGaN. Recent theoretical studies⁴ of the electronic band structure of w -BGaN, which are based on the local coherent potential approximation, predicted a decrease for $E_g(x)$ with x for small fractions of boron ($x < 20\%$). Still, no indication of the value of the bandgap bowing parameter C was given in Ref. 4, and the question about the bandgap bowing in BGaN remained open until now. In this letter we investigated the bandgap variation in BGaN films. The bowing effect is found to be strong, and it overwhelms the linear interpolation trend between the bandgaps of w -BN and GaN.

BGaN films with a wurtzite structure and different compositions of boron from 0% to 1.8% were grown on the c -axis oriented AlN/sapphire template substrates in a T -shape

low-pressure MOVPE reactor.⁵ We described the optimized growth procedures for boron-containing nitrides in Ref. 6. The growth temperature was 1000 °C. Trimethylgallium, triethylboron, and ammonia were used as precursors. The typical thickness of the grown BGaN layers d was 600 nm. The maximum composition of boron (1.8%) in BGaN was limited by both the phase separation in the solid phase and the surface saturation caused by the boron precursor. Epiready template substrates of 0.63- μ m-thick AlN layers on sapphire were chosen to enable the optical characterization of BGaN layers, which otherwise would experience an overlap with the bandgap and lattice parameters of conventional GaN/sapphire substrates. The boron content and strain in $B_xGa_{1-x}N$ layers were determined by x-ray diffraction (XRD) using end-point lattice parameters for w -BN ($c=0.417$ nm and $a=0.255$ nm) and w -GaN ($c=0.5185$ nm and $a=0.3189$ nm).⁷⁻⁹

Philips X'Pert diffractometer was utilized for XRD measurements of the in-plane and out-of-plane lattice mismatch for BGaN layers with respect to AlN. θ - 2θ profiles for symmetric (0 0 2) reflection are shown in Fig. 1(a) with the BGaN peaks at the left and the AlN peak at the right. The angular separation between the two peaks corresponds to the out-of-plane lattice mismatch between the two materials. The reciprocal space maps (RSMs) measured at the asymmetric (1 1 4) reflection demonstrate a significant degree of relaxation in BGaN layers with respect to AlN [Fig. 1(b)]. RSMs are dominated by the BGaN and AlN peaks, which are offset in the horizontal direction, with the shift corresponding to the in-plane lattice mismatch. Both in-plane and out-of-plane lattice parameters of BGaN layers depend on x , as presented in Fig. 2, in terms of the reciprocal lattice vectors q_x and q_z . Since the relaxation degree in our layer is very high varying between 70% and 90%, in the following we assume that the films are fully relaxed. A significant increase in the full width at half maximum (FWHM) for the rocking curves measured at the (0 0 2) reflection of BGaN corresponds to the increas-

^{a)}Electronic mail: aougazza@georgiatech-metz.fr.

^{b)}Electronic mail: sirenko@njit.edu.

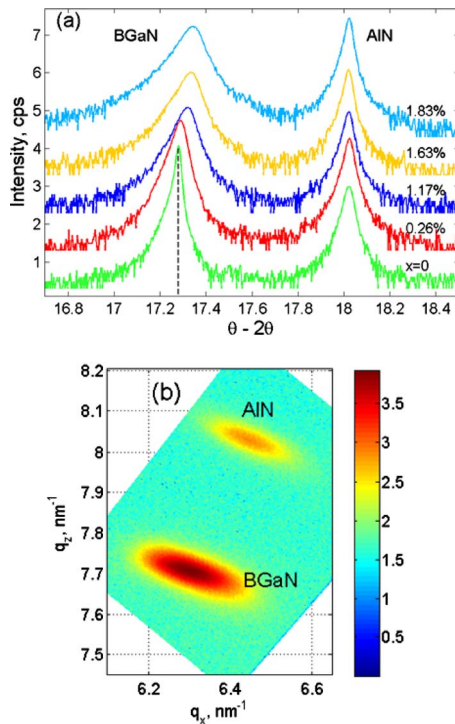


FIG. 1. (Color online) (a) XRD intensity for symmetric (0 0 2) reflection for five BGaN films grown on AlN/sapphire template substrate. Curves are vertically offset for clarity. Boron composition is shown next to the curves. Dashed vertical line indicates the position of the GaN diffraction peak. (b) RSM for (1 1 4) reflection of $B_{0.0026}Ga_{0.9974}N$ and AlN.

ing mosaicity of the samples with an increase in the boron content (Fig. 2, right scale). Thus, the XRD measurements demonstrate that our samples are relaxed and the main effect on the bandgap variation should originate not from any possible remains of the epitaxial strain between BGaN and AlN but from the group-III composition variation in the $B_xGa_{1-x}N$ layers.

Optical spectroscopy^{10,11} was utilized to investigate the bandgap variation in the BGaN layers. Transmission $T(\lambda)$ and reflection $R(\lambda)$ spectra were measured at room temperature with a Perkin Elmer LAMBDA 950 spectrophotometer. Figure 3 shows transmission spectra for the AlN/sapphire template substrate and five different compositions of the BGaN/AlN/sapphire samples. All spectra exhibit a well-

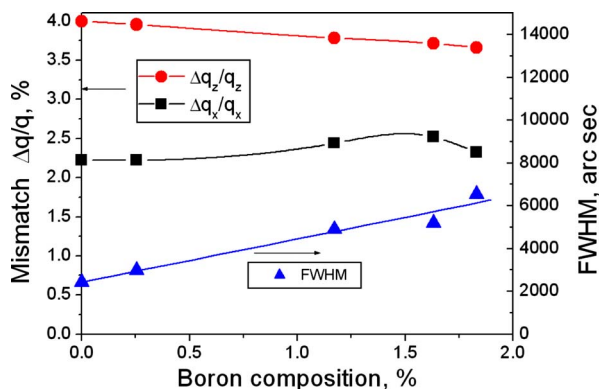


FIG. 2. (Color online) In-plane (circles) and out-of-plane (squares) variation in the lattice mismatch for BGaN layers determined with respect to the lattice parameters for unstrained AlN substrate (left scale). Triangles show the FWHM values for the rocking curves of BGaN (0 0 2) diffraction peak (right scale). Curves guide the eyes.

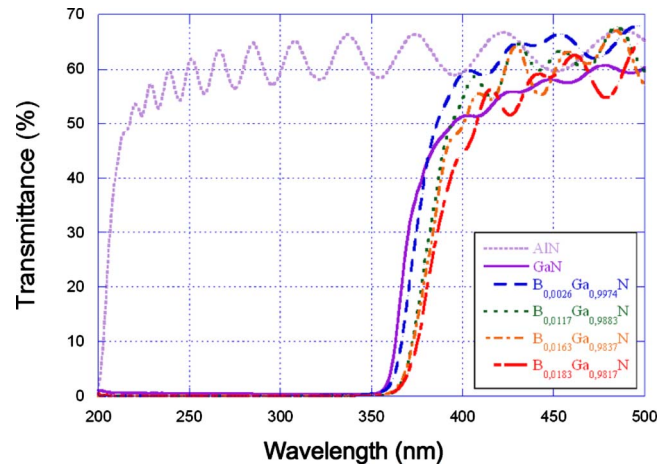


FIG. 3. (Color online) Transmission spectra of the $B_xGa_{1-x}N$ films grown with different boron composition x on AlN/sapphire template substrates.

defined transmission threshold at the bandgap that shifts to higher wavelengths with an increase in x . In addition, this trend is qualitatively confirmed using PL measurements shown in Fig. 4(b), but the inhomogeneous broadening of the PL spectra caused by defects is too high for quantitative analysis. Absorbance spectra $\alpha^2(\lambda)$, which are more accurate than PL for studies of the bandgap variation, are shown in Fig. 4(a). They have been obtained from transmission and reflection data as $\alpha(\lambda) = (1/d) \ln\{[1 - R(\lambda)]/T(\lambda)\}$. In principle, the intersection between the linear interpolation of the absorbance spectra and the wavelength axis should correspond to the optical bandgap, which is illustrated in Fig. 4(a), for the absorbance spectrum of GaN with a dashed line. However, in the case of more disordered BGaN layers with a tail of absorbance below the bandgap, the uncertainty of this approach is too high for precise measurements of the bowing parameter. To be more quantitative, transmission and reflection spectra were simulated using SCOUT2 software, which

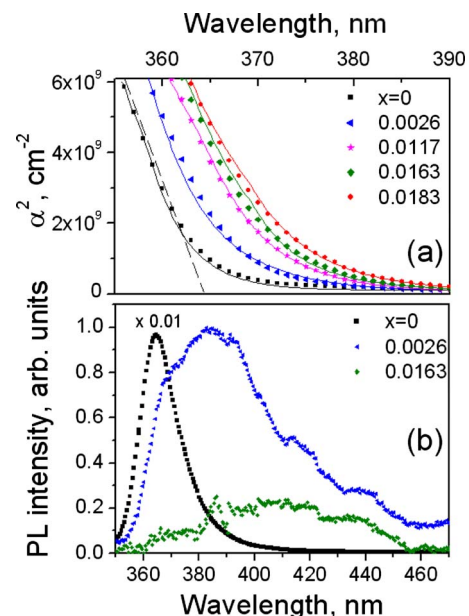


FIG. 4. (Color online) (a) Absorbance spectra of the $B_xGa_{1-x}N$ films for the same samples as in Fig. 3. Results of the fit are shown with solid curves. Straight dashed line interpolates the linear part of the absorbance spectrum for GaN. (b) PL spectra for GaN and two BGaN films.

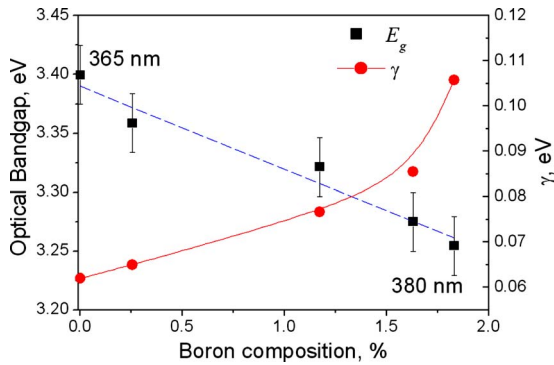


FIG. 5. (Color online) Bandgap variation (left axis) and inhomogeneous broadening of the bandgap (right axis) in B GaN thin films. Blue dashed curve shows a fit result to the experimental data for the bandgap bowing parameter $C=9.2$ eV.

has an option to calculate the optical response of semiconductors based on an O'Leary–Johnson–Lim (OJL) dielectric function model¹² for disordered systems using parabolic bands, with tail states exponentially decaying into the bandgap as $\exp[(\hbar\omega - E_g)/\gamma]$. In the dielectric function model for the B GaN layers, we included inhomogeneous broadening γ and the bandgap $E_g(x)$ as fitting parameters, while dielectric properties of the composite AlN/sapphire substrate were experimentally determined from independent reference measurements. The results of the fit are shown in Fig. 4(a). This approach allowed us to decouple two contributions to the bandgap absorption threshold, which originate from (i) the disorder and (ii) the composition-induced renormalization of the bandgap $E_g(x)$. The first contribution is described by the parameter γ , which increases with the boron content (Fig. 5), and as expected, it correlates with the FWHM values for the XRD rocking curves (Fig. 2). The summary for the composition-induced redshift of $E_g(x)$ is shown in Fig. 5. This trend does not support the interpolated linear dependence between the bandgaps of w -GaN and w -BN and can be only understood using the bandgap bowing concept. The bandgap fits well as $E_g(x) = xE_g^{w\text{-BN}} + (1-x)E_g^{w\text{-GaN}} - Cx(1-x)$ with the bowing parameter $C=9.2 \pm 0.5$ eV, the optical gap of GaN of $E_g^{w\text{-GaN}}=3.39$ eV, and the bandgap of w -BN $E_g^{w\text{-BN}}=5.5$ eV.^{7,8} Note that the exact value for $E_g^{w\text{-BN}}$ has not yet been established, and for example, Ref. 13 reports a higher value of 5.81 eV. Still, for our boron compositions ($x < 2\%$), this uncertainty in $E_g^{w\text{-BN}}$ corresponds to a systematic error of C that is five times less than the experimental accuracy of our measurement (± 0.5 eV). We can compare $C=9.2 \pm 0.5$ eV with the recommended bowing parameters for ternary nitride-based systems with the wurtzite structure, which have been summarized in Refs. 14 and 15: $C=1$ eV for AlGaIn, $C=3$ eV for InGaIn, and for lesser known InAlIn the value of C varies in literature between 7 and 16 eV. A relatively large value of C in B GaN, which can be traced to the disorder effects produced by the presence of different group-III elements,¹⁶ can be attributed to the high contrast between the average bond length for B–N and Ga–N. Figure 6 illustrates the general trend for the bandgap bowing parameters in ternary nitride compounds by presenting experimental C values versus the lattice mismatch between the end-point binaries. Thus, our experimental value of 9.2 ± 0.5 eV is in a reasonable range of the bowing parameters for ternary nitride compounds.

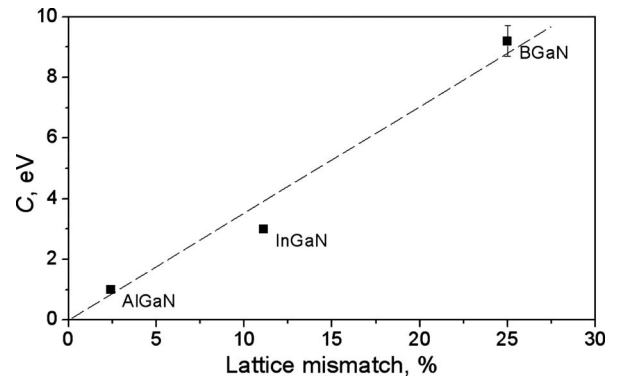


FIG. 6. Bandgap bowing parameters for ternary nitride compounds with a wurtzite structure vs the lattice mismatch between the end-point binary compounds. Data for AlGaIn and InGaIn are from Ref. 14. Dashed line guides the eyes.

In conclusion, for the B GaN films obtained in the limit of boron solubility in GaN, the bowing effect is stronger than the linear interpolation trend between the bandgaps of GaN and BN. This result will be important for bandgap engineering of optoelectronic devices based on B GaN. Considering the observed bowing effect in B GaN, one can expect a similar behavior in B InN and B AlN. Additional studies of elastically strained layers of B GaN and piezoinduced variation in the bandgap will be required for the complete description of this important ternary compound.

The authors gratefully acknowledge C. Bazin for the help with the transmission measurements.

- ¹W. A. Harrison, *Electronic Structure and the Properties of Solids: The Physics of the Chemical Bond* (Dover, New York, 1989).
- ²H. Kawanishi, M. Haruyama, T. Shirai, and Y. Suematsu, *Proc. SPIE* **2994**, 52 (1997).
- ³T. Honda, M. Shibata, M. Kurimoto, M. Tsubamoto, J. Yamamoto, and H. Kawanishi, *Jpn. J. Appl. Phys., Part 1* **39**, 2389 (2000).
- ⁴V. V. Ilyasov, T. P. Zhadanova, and I. Ya. Nikiforov, *Phys. Solid State* **48**, 654 (2006).
- ⁵S. Gautier, C. Sartel, S. Ould-Saad, J. Martin, A. Sirenko, and A. Ougazzaden, *J. Cryst. Growth* **298**, 428 (2007).
- ⁶A. Ougazzaden, S. Gautier, C. Sartel, N. Maloufi, J. Martin, and F. Jomard, *J. Cryst. Growth* **298**, 316 (2007).
- ⁷S. L. Rumyantsev, M. E. Levinshtein, A. D. Jackson, S. N. Mohammad, G. L. Harris, M. G. Spencer, and M. S. Shur, in *Properties of Advanced Semiconductor Materials GaN, AlN, InN, BN, SiC, SiGe*, edited by M. E. Levinshtein, S. L. Rumyantsev, and M. S. Shur (Wiley, New York, 2001), pp. 67–92.
- ⁸V. Bougrov, M. E. Levinshtein, S. L. Rumyantsev, and A. Zubrilov, in *Properties of Advanced Semiconductor Materials GaN, AlN, InN, BN, SiC, SiGe*, edited by M. E. Levinshtein, S. L. Rumyantsev, and M. S. Shur (Wiley, New York, 2001), pp. 1–30.
- ⁹V. Darakchieva, B. Monemar, and A. Usui, *Appl. Phys. Lett.* **91**, 031911 (2007).
- ¹⁰M. D. McCluskey, C. G. Van de Walle, L. T. Romano, B. S. Krusor, and N. M. Johnson, *J. Appl. Phys.* **93**, 4340 (2003).
- ¹¹M. Androulidaki, N. T. Pelekanos, K. Tsagaraki, E. Dimakis, E. Iliopoulos, A. Adikimenakis, E. Bellet-Amalric, D. Jalabert, and A. Georgakilas, *Phys. Status Solidi C* **3**, 1866 (2006).
- ¹²S. K. O'Leary, S. R. Johnson, and P. K. Lim, *J. Appl. Phys.* **82**, 3334 (1997).
- ¹³Y.-N. Xu and W. Y. Ching, *Phys. Rev. B* **44**, 7787 (1991).
- ¹⁴I. Vurgaftman, J. R. Meyer, and L. R. Ram-Mohan, *J. Appl. Phys.* **89**, 5815 (2001).
- ¹⁵T. Peng, J. Piprek, G. Qiu, J. O. Olowolafe, K. M. Unruh, C. P. Swann, and E. F. Schubert, *Appl. Phys. Lett.* **71**, 2439 (1997).
- ¹⁶J. A. Van Vechten and T. K. Bergstresser, *Phys. Rev. B* **1**, 3351 (1970).